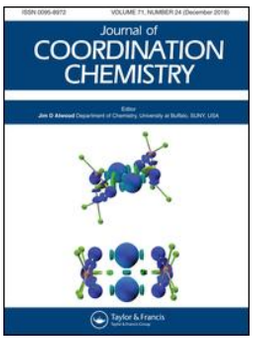

Journal of Coordination Chemistry

ISSN: 0095-8972 (Print) 1029-0389 (Online) Journal homepage: https://www.tandfonline.com/loi/gcoo20

Synthesis, antiproliferative activity and mechanism of copper(II)-thiosemicarbazone complexes as potential anticancer and antimicrobial agents

Jinxu Qi, Xuejiao Wang, Taichen Liu, Martha Kandawa-Schulz, Yihong Wang & Xinhua Zheng

To cite this article: Jinxu Qi, Xuejiao Wang, Taichen Liu, Martha Kandawa-Schulz, Yihong Wang & Xinhua Zheng (2020): Synthesis, antiproliferative activity and mechanism of copper(II)-thiosemicarbazone complexes as potential anticancer and antimicrobial agents, Journal of Coordination Chemistry, DOI: 10.1080/00958972.2020.1768378

To link to this article: https://doi.org/10.1080/00958972.2020.1768378

JOURNAL OF COORDINATION CHEMISTRY
https://doi.org/10.1080/00958972.2020.1768378

Taylor & Francis
Taylor & Francis Group

Synthesis, antiproliferative activity and mechanism of copper(II)-thiosemicarbazone complexes as potential anticancer and antimicrobial agents

Jinxu Qi[a#], Xuejiao Wang[b#], Taichen Liu[a], Martha Kandawa-Schulz[c], Yihong Wang[b] and Xinhua Zheng[a]

[a]School of Medicine, Pingdingshan University, Pingdingshan, China; [b]School of Chemistry and Chemical Engineering, Southeast University, Nanjing, China; [c]Department of Chemistry and Biochemistry, University of Namibia, Windhoek, Namibia

ABSTRACT

Malignant tumors have become one of the challenges to global human health today, and the development of new drugs has become a research hotspot for tumor treatment. In order to prove that copper(II)-thiosemicarbazone complexes can be used as antibacterial and antitumor agents, we have synthesized and characterized three copper(II) complexes (**C1**-**C3**). These Cu(II) complexes exhibited excellent anticancer and antimicrobial activity, and greatly exceed the corresponding metal-free ligands. **C3** has the highest anti-proliferative activity ($0.20 \pm 0.04\,\mu M$) against A549 (human lung carcinoma cell lines) and the best inhibitory zone diameter (25.78 ± 0.18 mm) against *E. coli*. The lipophilicity of the ligand is closely related to the anti-proliferative and antibacterial activities of these Cu(II) complexes. The study of the cellular mechanism demonstrates that these Cu(II) complexes promoted cell apoptosis by catalyzing hydrogen peroxide to produce intracellular reactive oxygen species (ROS). Antibacterial experiments showed that these Cu(II) complexes exhibited potent antibacterial activities, especially against gram-negative bacteria. These Cu(II) complexes may initially cause outer membrane/lipopolysaccharide (LPS) instability, disrupt cell membranes, and ultimately lead to bacterial cell lysis.

ARTICLE HISTORY
Received 16 February 2020
Accepted 1 May 2020

KEYWORDS
Copper complex; thiosemicarbazone; anticancer activity; antimicrobial activity; apoptosis

CONTACT Yihong Wang Yihongwang@Seu.edu.cn; Xinhua Zheng zhengxinhua70@163.com
#Jinxu Qi and Xuejiao Wang equally contributed to this study.

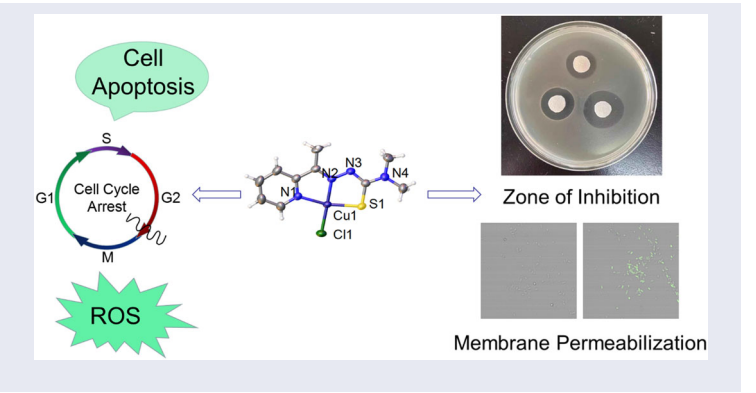

1. Introduction

Malignant tumors are common and frequently-occurring diseases that seriously endanger human health in modern life [1–3]. After Rosenberg *et al.* [4] found that cisplatin(II) is a better drug for cancer, a series of new platinum drugs have been developed one after another, but they still show strong renal toxicity, ototoxicity and neurotoxicity in clinical trials [5–8]. Therefore, this has also led to research interest in new metal-based antitumor drugs [9–13]. At the same time, many patients with malignant tumors have low immune function or long-term use of chemotherapeutic drugs, resulting in neutrophil reduction or even deficiency, which causes pathogenic bacterial infections in the body [14, 15]. In order to take into account the complications of microbial infection caused by the treatment of malignant tumors, the development of new drugs with strong antitumor activity and strong antibacterial activity is also a new direction for the research of antitumor drugs.

Copper is an important part of human proteins and enzymes. Many important enzymes require a small amount of copper to participate and activate [16, 17]. Due to their higher proliferation rate, tumor cells usually require more copper than normal cells [18]. In recent years, the high activity of copper-based complexes in cancer cells has been studied in depth [13, 19–21]. Thiosemicarbazone derivatives and their complexes with metals have significant antiviral, antituberculous, antibacterial and antitumor activities [22–25]. Therefore, it is of great theoretical and practical significance to design and synthesize thiosemicarbazone ligands and copper complexes of various compositions and structures, and explore the anticancer, antibacterial activity, and mechanism of action of these compounds.

Herein, we synthesized and characterized three Cu(II) thiosemicarbazone complexes. To evaluate the antitumor mechanism of copper(II) complexes, we studied their antiproliferative activity, apoptosis analysis, intracellular reactive oxygen species (ROS), and cell cycle. Meanwhile, the antibacterial mechanism of Cu(II) complexes was studied by antibacterial activity, inhibition zone diameters and cell membrane permeability.

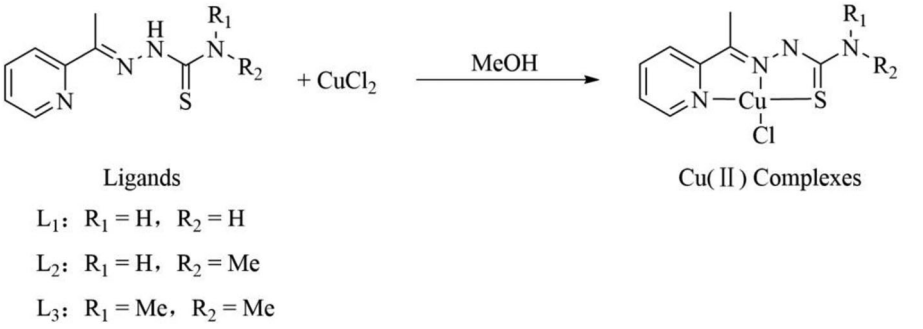

Scheme 1. Synthesis routes for **C1**-**C3**.

2. Experimental

2.1. Materials and methods

All chemical reagents were supplied by Innochem Company (Shanghai, China) and were of analytical grade as well as were used without additional purification. Water used in the reactions was distilled prior to use. Human lung carcinoma cell lines A549 and human colon cancer cell lines Caco-2 were obtained from Chinese Academy of Sciences.

2.2. Synthesis and characterization of Cu(II) complexes

The ligands (L1-L3) were synthesized according to the description in our published reference [26]. 2-Acetylpyridine (1 mole equivalent) and acetic acid glacial (5 drops) were placed in a round-bottom flask to which ethanol (10 mL) and thiosemicarbazide (1 mM) were added. The solution was heated under refluxed for 4 h. The precipitate formed was collected by vacuum filtration, washed three times with cold ethanol and dried in a vacuum desiccator.

Cu(II) complexes (**C1**, **C2**, and **C3**) were synthesized following the previous description [20, 27, 28]. One mole equivalent of $CuCl_2$ was added to methanol solution of thiosemicarbazone (10 mL, 1 mM) and stirred, stand and allow the solvent to evaporate to gradually precipitate the Cu(II) complex single crystals. The precipitate was collected by filtration and washed with ice-cold ethanol and dried *in vacuo* overnight. The synthesis process is shown in Scheme 1.

[2-[1-(2-Pyridinyl)ethylidene]hydrazinecarbothioamide-N,N,S-copper(II)] chloride (**C1**): yield 74%. Anal. Calcd for $C_8H_{10}Cl_2CuN_4S$: C, 29.23; H, 3.07; N, 17.04. Found: C, 29.18; H, 3.11; N, 17.09. MS m/z (%) 291.95 (M–Cl, 100).

[N-methyl-2-[1-(2-pyridinyl)ethylidene]hydrazinecarbothioamide-N,N,S-copper(II)] chloride (**C2**): yield 78%. Anal. Calcd for $C_9H_{11}ClCuN_4S$: C, 35.29; H, 3.62; N, 18.29. Found: C, 35.22; H, 3.66; N, 18.21. MS m/z (%) 270.0 (M–Cl, 100).

[N,N-dimethyl-2-[1-(2-pyridinyl)ethylidene]hydrazinecarbothioamide-N,N,S-copper(II)] chloride (**C3**): yield 76%. Anal. Calcd for $C_{10}H_{13}ClCuN_4S$: C, 37.50; H, 4.09; N, 17.49. Found: C, 37.42; H, 4.02; N, 17.41. MS m/z (%) 320.29 (M–Cl, 100).

Table 1. Crystal data and structure refinement for C1-C3.

Complexes	C1	C2	C3
Empirical formula	$C_8H_{10}Cl_2CuN_4S$	$C_9H_{11}ClCuN_4S$	$C_{10}H_{13}ClCuN_4S$
Formula weight	328.7	306.27	320.29
Temperature/K	296.15	296.15	296.15
Crystal system	Monoclinic	Monoclinic	Monoclinic
Space group	$P2_1/c$	$P2_1/n$	$P2_1/n$
a/Å	11.0147(9)	8.029(8)	11.338(7)
b/Å	9.5131(4)	15.917(17)	9.512(6)
c/Å	12.3311(10)	9.133(10)	12.350(8)
α/°	90	90	90
β/°	112.051(9)	92.378(19)	104.611(10)
γ/°	90	90	90
Volume/Å^3	1197.59(14)	1166(2)	1288.8(14)
Z	4	4	4
F(000)	660	620	652
Index ranges	$-13 \leq h \leq 13$ $-11 \leq k \leq 11$ $-15 \leq l \leq 14$	$-10 \leq h \leq 10$ $-19 \leq k \leq 19$ $-11 \leq l \leq 11$	$-14 \leq h \leq 14$ $-11 \leq k \leq 12$ $-15 \leq l \leq 15$
Goodness-of-fit on F^2	1.078	1.019	1.074
Final R indexes [$I \geq 2\sigma$ (I)]	$R_1 = 0.0281$, $wR_2 = 0.0703$	$R_1 = 0.0332$, $wR_2 = 0.0722$	$R_1 = 0.0270$, $wR_2 = 0.0715$
Final R indexes [all data]	$R_1 = 0.0370$, $wR_2 = 0.0749$	$R_1 = 0.0540$, $wR_2 = 0.0807$	$R_1 = 0.0344$, $wR_2 = 0.0759$
CCDC NO.	1976432	969493	1055568

2.3. Determination of structure of Cu(II) complexes

Crystallographic data were collected at 296.15 K on a Bruker SMART Apex II CCD diffractometer employing Mo-Kα radiation (λ = 0.71073 Å) source. Data reduction and empirical absorption corrections (multiscan) were performed with Oxford Diffraction CrysAlisPro software. All structures were solved by direct methods with Olex2 and refined by full-matrix least-squares methods with Olex2 software [29]. All non-H atoms were refined anisotropically using the riding model to fix the H atom in a geometrically ideal position. Molecular structure diagrams were produced with Olex2 software [29]. The crystal data of Cu(II) complexes are exhibited in Table 1. Selected bond lengths and angles are shown in Tables S1–S6.

2.4. Cytotoxicity assay (MTT)

In this study, MTT (3-(4,5-dimethyl-2-thiazolyl)-2,5-diphenyl-2H-tetrazolium bromide) assay [30] was used to examine the cytotoxicity of cells. At 37 °C, the cell lines were grown in an incubator (ThermoFisher) with 95% air and 5% CO_2. Thiosemicarbazide ligands and Cu(II) complexes were dissolved in DMSO as 10 mM stock solutions. Stock solutions in DMSO were diluted to a concentration of <0.1% in cell culture medium to avoid the solvent effect on cell proliferation. Cells were seeded in 96-well plates and allowed to adhere overnight in an incubator at 37 °C. The seeding densities used were 5 × 104 cells/well. Different concentrations (0, 1, 2.5, 5, 10 μM) of ligands and their Cu(II) complexes were added to the plates and incubated for 48 h/37 °C. 20 μL MTT (5 mg/mL) was added to the cells and incubated for another 4 h. Finally, DMSO (100 μL) was added, and the optical density (OD) of living cells was recorded at a wavelength of 570 nm. MTT color formation was directly proportional to the number of viable cells, validating its use in these studied. The half-maximum inhibitory

concentration (IC_{50}) values were processed and analyzed according to the nonlinear multi-purpose curve fitting program GraphPad Pris.

2.5. Cell cycle distribution analysis

The A549 cells were seeded in 70-mm culture dishes at a density of 1×105 cells/mL and incubated at 37 °C for 24 h. Then, the medium was removed and freshly prepared solutions of the tested compounds, **C1**, **C2** and **C3**, at a 1 μM concentration were added. After 24-h treatment, cells were harvested and washed 3 times with ice-cold PBS. Then, the cells were fixed in ice cold 75% ethanol and stored at -20 °C for 12 h, as well as rinsed with cold PBS. The RNase (Ribonuclease, 2.5 mg/ml) was added to the cells for culture and stained with pyridinium iodide (PI, 50 mg/mL) for 0.5 h, followed by flow cytometry (BD, Accuri™ C6) analysis. The 10,000 events for each sample were recorded and the data was resolved by MFLT32 software.

2.6. Cell apoptosis assay

The A549 cell apoptotic events induced by **C1**, **C2** and **C3** were determined by Annexin V and PI staining according to the manufacturer's protocol for the Annexin V-FITC Apoptosis Detection Kit (Bection Dickinson). At 5% CO_2/95% air and 37 °C, 2 mL 1×106 cells/mL were used for incubation with **C1**, **C2** and **C3** (1 μM) for 24 h. The A549 cells were suspended in 300 μL of mixed buffer (140 mM NaCl, 10 mM Hepes/NaOH, 2.5 mM $CaCl_2$, pH 7.4), and then 5 μL each of PI and Annexin V were added to these samples. Then, samples incubated at room temperature for 20 min were determined by flow cytometry analysis (BD, Accuri™ C6), and the rate of apoptosis was analyzed by FlowJo software.

2.7. Intracellular ROS measurements

Evaluation of intracellular ROS was performed by the procedure of active oxygen assay kit (Beyotime, Suzhou) and flow cytometry. The A549 cells were treated with **C1**, **C2** or **C3** (5 μM) for 30 min at 37 °C. 2′,7′-Dichlorodihydro-fluorescein diacetate (H_2DCF-DA) was added to the cells for 0.5 h and then washed twice with ice-cold PBS. Cells were collected for flow cytometry assessment (BD, AccuriTM C6). Data analysis was performed using FlowJo software.

2.8. Antimicrobial assays

In vitro antimicrobial activity of the compounds was tested by the standard serial dilution method against four bacterial strains i.e. Gram-positive bacteria *Staphylococcus aureus* and *Staphylococcus epidermidis* (*S. aureus* ATCC 29213, *S. epidermidis* ATCC 14990), Gram-negative bacteria *Escherichia coli* and *Pseudomonas aeruginosa* (*E. coli* ATCC 25922, *P. aeruginosa* ATCC 27853), which were cultured on nutrient broth and potato dextrose broth as nutrient medium.

Stock solutions of thiosemicarbazide ligands and Cu(II) complexes were serially diluted two-fold from 512 to 1 μM/mL in Mueller-Hinton (MH) broth. 100 μL of each dilution and 100 μL of bacterial suspension at 1 × 106 cells/mL (OD_{540} value of 1.0 is equivalent to the density of 10^9 cells/mL) were transferred into the wells of a microplate, respectively. The negative control (media only) and positive control (bacteria without inhibitors) on the same plate were used as references to determine the growth inhibition of bacteria. All the plates were covered and incubated at 37 °C for 18 h without shaking. After incubation, the minimal inhibitory concentrations (MICs) were determined by the lack of turbidity in the wells. The minimum bactericidal concentrations (MBCs) were measured by spreading 100 μL of solution from each clear well (≥ MIC) onto agar plates. The agar plates were kept in an incubator at 37 °C for 24 h. the MBC was determined as the lowest concentration with no colonies had formed corresponded.

2.9. Inhibition zone tests

Antibacterial studies are revealed by analyzing thiosemicarbazone ligands and Cu(II) complexes by disk diffusion method. 100 μL of cell suspension was spread over the sterilized agar plate with the use of a sterilized spreader, and pasted a filter paper containing 2MICs antibacterial drug **C1**-**C3** on the surface of the agar inoculated with the test bacteria. The plates were then incubated at 37 °C/16 h in the incubator. Following the incubation period, the inhibition zone was considered in millimeter (mm) [31, 32].

2.10. Membrane permeability study

As described above, the Sytox green uptake assay was performed [33]. *S. aureus* and *E. coli* were incubated for 12 h, washed twice with cold PBS, centrifuged and resuspended to form a 2 × 107 cfu/mL solution. Cells were fixed on glass slides coated with poly (L-lysine) by incubation with Cu(II) complexes at 2 MICs for 0.5 h at 30 °C. The slides were washed with PBS and incubated with 5 μM Sytox green dye in a dark environment at 30 °C for 30 minutes. Finally, the slide was washed again with PBS and analyzed with a confocal microscope (Olympus FV3000) at an excitation wavelength of 485 nm. Samples containing only bacteria and Sytox green dye as blank controls.

2.11. Statistical analysis

Experiment data were compared using Student's test. Results were expressed as mean ± SD (number of experiments) and considered to be statistically significant when $p < 0.05$. All experiments were repeated at least three times.

3. Results and discussion

3.1. Synthesis and crystal structure description

According to the method reported in the literature, the ligands L1-L3 were directly prepared by Schiff base condensation reaction, and the purity of the obtained ligand

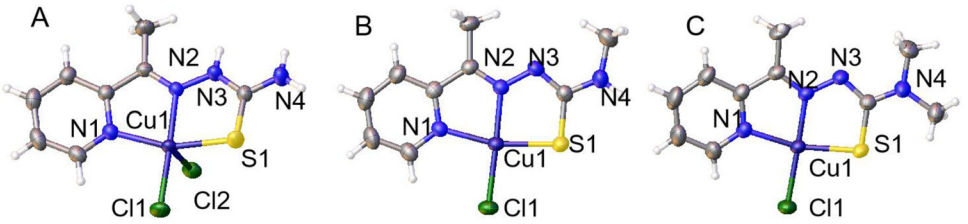

Figure 1. Molecular structure of Cu(II) complexes showing the environment about the Cu(II) atom. (A) **C1**; (B) **C2**; (C) **C3**.

product was high without further purification [26, 34, 35]. The coordination of the ligand with copper chloride produced a ligand/Cu(II) complex of 1:1 (Figure 1). All Cu(II) complexes were crystallized from methanol solution, and the structures were identified by single-crystal X-ray diffractometer.

The crystal data of the three Cu(II) complexes are shown in Table 1, and the bond lengths and angles are listed in Tables S1–S6. Although the ligands are similar in structure, the Cu(II) complexes are not. Complex **C1** contains neutral thiosemicarbazone ligand and adopts a square-pyramidal geometry, while the other compounds contain anionic deprotonated thiosemicarbazone ligands and crystallize in square-planar geometries. Certainly, the apical chlorido Cl2 ligand in **C1** exhibits a bond length with Cu(II) longer than the Cu-Cl1 due to the Jahn-Teller effect, but the bond remains. **C1**-**C3** are all monoclinic, but the space group to which **C1** belongs is $P2_1/c$, and the space group to which **C2** and **C3** belong is $P2_1/n$. The Cu(II) metal center of **C1** is coordinated by two N atoms (N1 and N2), one Cl atom (Cl1) and one S atom forming an approximately planar structure (Figure 1). Due to coordination with Cu(II), most of the ligand atoms (N1-N4 and C1-C9) are fixed on the approximate plane. The bond angles of N1-Cu1-Cl1, Cl1-Cu1-S1, S1-Cu1-N2 and N1-Cu1-N2 with Cu(II) as the center are 99.41°, 96.41°, 84.35° and 79.11°, respectively. The lengths of Cu1-N1 (= 2.029(2) Å) and Cu1-N2 (= 1.9783(18) Å) are similar. There is no significant difference in the length of Cu1-Cl1 (= 2.2864(7) Å) and Cu1-S2 (= 2.2243(7) Å) bonds. The bond angles and bond lengths in **C2** and **C3** are similar to **C1**. In **C2** and **C3**, the anion Cl and tridentate thiosemicarbazone coordinate with the central copper(II) ion to form an approximately planar structure. The bond length, bond angle and coordination environment of **C2** match the published results [36, 37].

3.2. In vitro cytotoxic studies of ligands and Cu(II) complexes

Scientists have deeply studied thiosemicarbazone analogs and proved that these ligands and complexes have significant antitumor activity [37–49]. Their research focuses on SK-N-MC Neuroepithelioma Cells, SK-Mel-28 melanoma, *etc.*; our experimental results are complementary to their experimental results. Numerous reports indicate that thiosemicarbazone ligands have significant activity against tumors, such as breast cancer, liver cancer, lung cancer, colon cancer, etc. [18, 34, 50]. The antiproliferative properties of the thiosemicarbazone ligands and Cu(II) complexes on two malignant cancer cell lines (human lung cancer cell lines A549, human colon cancer cell lines Caco-2) were evaluated, as shown in Table 2. The anticancer activity of L3 was significantly higher than that of L1 and L2. The results showed that the increased lipophilicity of the terminal-N

Table 2. IC_{50} Values of ligands and Cu(II) complexes toward cell lines for 48 h.

	IC_{50} ± SD (μM)	
Compounds	A549	Caco-2
L1	11.77 ± 0.78	86.89 ± 0.24
L2	8.04 ± 0.22	1.36 ± 0.27
L3	1.07 ± 0.38	0.75 ± 0.17
C1	0.22 ± 0.06	0.74 ± 0.51
C2	0.42 ± 0.15	1.07 ± 0.29
C3	0.20 ± 0.04	0.68 ± 0.14

substitution can enhance the antitumor activity of the compound. After 48 h of incubation, the antiproliferative activity of the Cu(II) complexes was significantly higher than that of the corresponding individual ligands, and the antitumor proliferative activity of **C1** was similar to **C3**. Results indicated that the antiproliferative activity of copper complexes is determined by the corresponding ligands, and the antitumor activity of the ligands is enhanced by coordination with copper. Since the Cu(II) complexes **C1**-**C3** exhibited better antitumor activities than the ligands, they were selected for further analyses.

3.3. Cell cycle analysis

Cell cycle arrest plays a vital role in preventing the malignant proliferation of tumor cells, of which G1/S and G2/M transitions are the most important stages of the cell cycle [51]. The effect of Cu(II) complexes on A549 cell cycle was evaluated by staining the DNA of A549 cells with pyridine iodide (PI) and analyzing them by flow cytometry (Figure 2). From the figure we can see that the percentage of G2 phase of cells treated with **C1**, **C2** and **C3** were reduced by 3.38%, 2.62% and 12.41%, respectively, compared with the control group. Data demonstrated the Cu(II) complexes can inhibit cell proliferation by inhibiting the G2/M phase transition in the cell cycle.

3.4. Cell apoptosis assay

Programmed cell death refers to the orderly death of cells controlled by genes in order to maintain internal environment stability [52]. However, apoptosis is usually suppressed in tumor cells, so activating apoptosis is an effective anticancer pathway [53]. After treating A549 cells with Cu(II) complexes for 12 h, staining with Annexin V-FITC/PI and analyzing the effect of complexes on promoting apoptosis by flow cytometry (Figure 3). According to the data **C1**, **C2** and **C3** induced early apoptosis of cells, which increased by 33.77%, 19.07% and 44.67% compared with the control group, respectively. The results of cell apoptosis assay proved that **C3** has a stronger ability to promote apoptosis, which was consistent with the results of MTT assay.

3.5. Intracellular ROS measurements

The intervention of some exogenous drugs will cause excessive production of reactive oxygen species (ROS) in the cell or reduce the ability to clear them, leading to apoptosis [54]. To assess whether Cu(II) complexes can induce increased intracellular ROS,

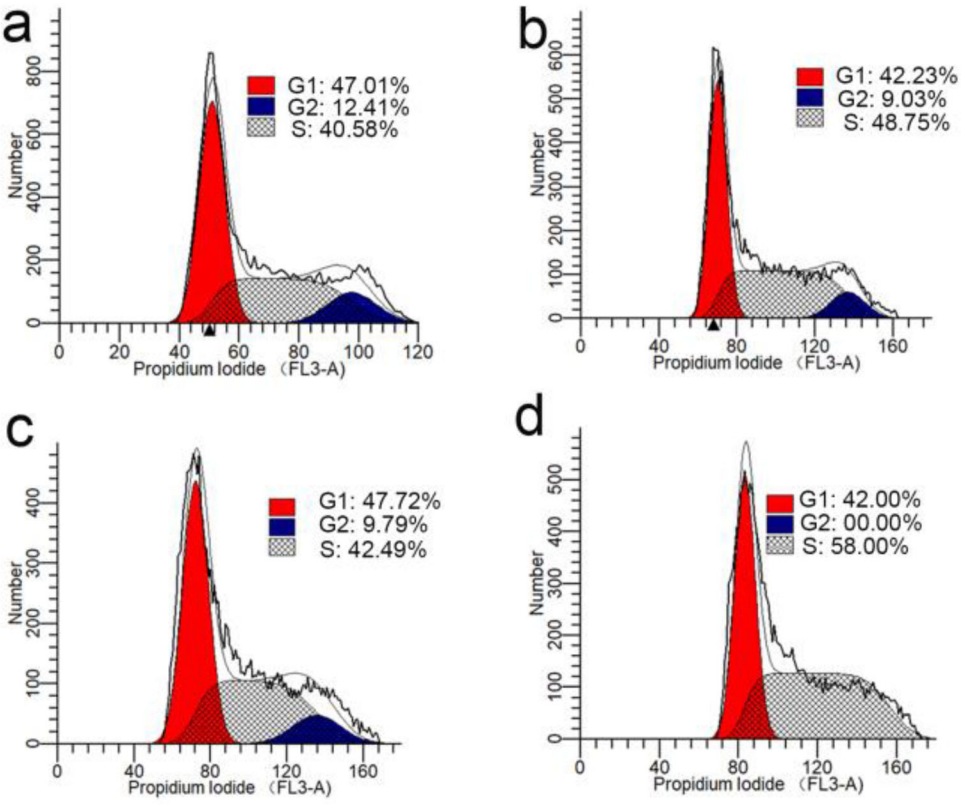

Figure 2. Effect of the cell cycle of A549 treated with (a) control, (b) **C1**, (c) **C2**, and (d) **C3**.

after co-incubating A549 with Cu(II) complexes for 48 h, they were stained with fluorescent probes (DCFH-DA) and analyzed by flow cytometry (Figure 4). Compared with the control, the intracellular ROS of the three drug-treated cells were significantly increased, and **C3** had the strongest ability to promote the production of ROS. Excessive intracellular ROS can inhibit G1, S, and G2 phase proliferation and combined with the above-mentioned cell cycle analysis, it can be found that G2/M phase block is related to antioxidative damage and antiapoptotic processes.

3.6. Antibacterial activity assays

The antibacterial activity of synthesized ligands and Cu(II) complexes were screened against two Gram-positive bacteria (*S. aureus* and *S. epidermidis*) and two Gram-negative bacteria (*E. coli* and *P. aeruginosa*). MIC and MBC are given in Table 3. Antibacterial activity data showed that under similar conditions, the antibacterial activity of metal complexes is higher than that of the corresponding ligands, and the ligands have little inhibition activity. Cu(II) complexes exhibited more antimicrobial activity to Gram-negative bacteria than Gram-positive bacteria. This is mainly due to the complexity of the cell wall structure of Gram-positive bacteria and Gram-negative bacteria. The lipid membrane facilitates the passage of any fat-soluble substance, and liposolubility is known to be an important factor in controlling antibacterial activity [55].

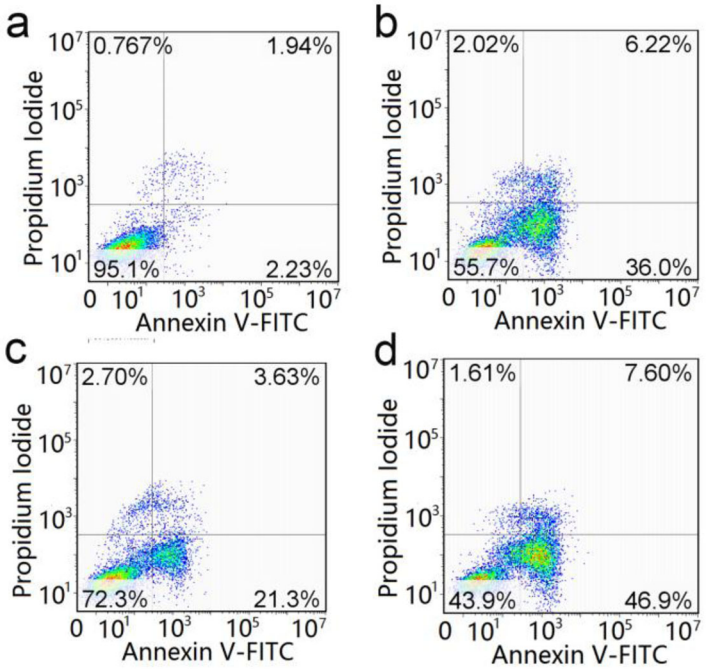

Figure 3. Effect of the cell apoptosis. Quantification of Annexin V and PI double-stained A549 cells after treatment with (a) control, (b) **C1**, (c) **C2**, and (d) **C3**, for 24 h at the indicated concentrations by flow cytometry.

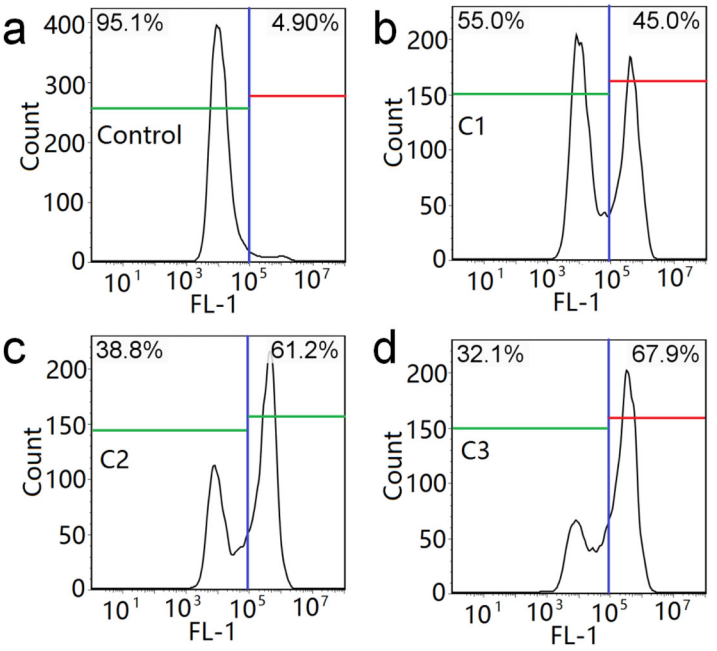

Figure 4. Intracellular ROS was detected in A549 cells after treatment with (a) control, (b) **C1**, (c) **C2**, and (d) **C3** for 24 h.

Table 3. Minimal inhibitory concentration (MIC) and minimal bactericidal concentration (MBC) of ligands and Cu(II) complexes.

	MIC (MBC) (μM)			
Compounds	*S. aureus* 29213	*S. epidermidis* 14990	*P. aeruginosa* 27853	*E. coli* 25922
L1	>256(>256)	>256(>256)	>256(>256)	>256(>256)
L2	>256(>256)	>256(>256)	>256(>256)	256(>256)
L3	128(>256)	256(>256)	256(>256)	128 (>256)
C1	128(256)	128(256)	128(256)	128(256)
C2	32(32)	32(32)	16(16)	16(32)
C3	16(32)	16(32)	8(16)	8(16)

Table 4. Zone of inhibition (in mm) against microorganisms (antimicrobial agent dose per disk is 2MICs).

Compounds	*S. aureus* 29213	*E. coli* 25922
L1	0	0
L2	0	12.22 ± 0.11
L3	0	13.74 ± 0.30
C1	14.00 ± 0.14	19.62 ± 0.07
C2	14.94 ± 0.03	21.68 ± 0.15
C3	15.52 ± 0.21	25.78 ± 0.18

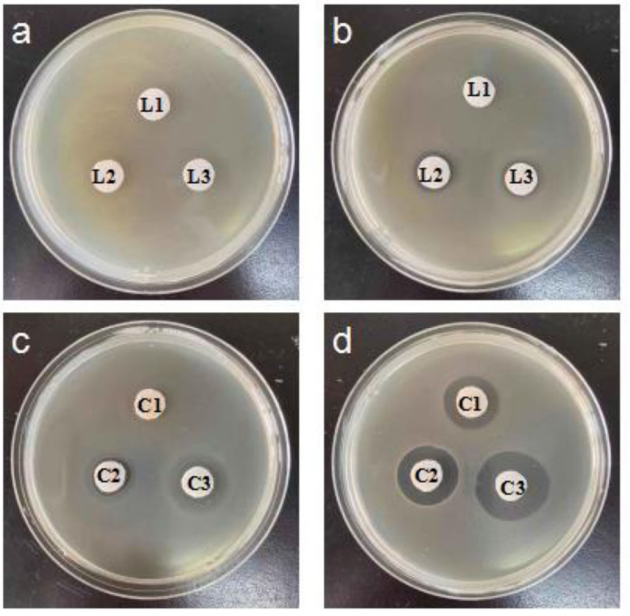

Figure 5. Zone of inhibition against microorganisms (a, c) *S. aureus*; (b, d) *E. coli*.

In order to further clarify the antibacterial effects of ligands and Cu(II) complexes on different bacteria, zone of inhibition tests were performed on *S. aureus* and *E. coli*. As shown in Table 4 and Figure 5, for *S. aureus*, the ligands did not show antibacterial activity over the considered strains since no inhibition zones were observed. For *E. coli*, the diameters of the inhibition zones of L2 and L3 were 12.22 ± 0.11 mm and 13.74 ± 0.30 mm, respectively. The diameters of the corresponding Cu(II) complexes

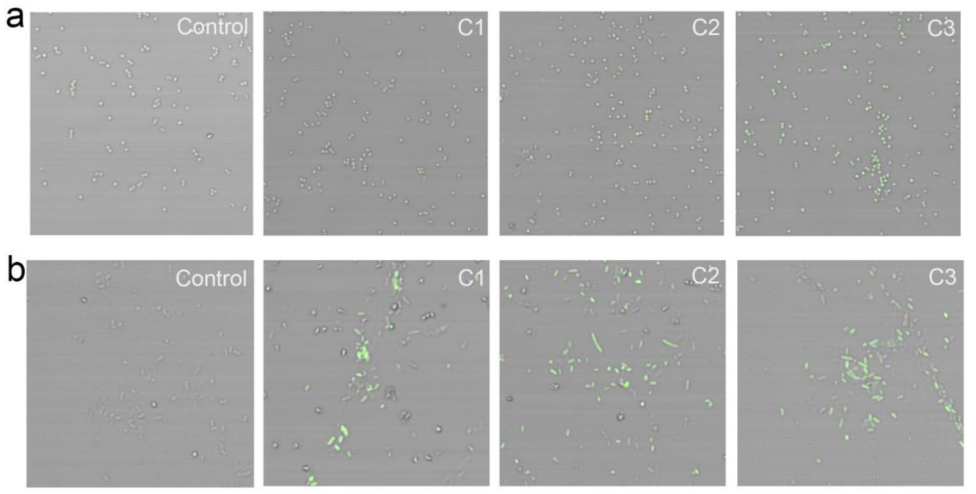

Figure 6. Complex-induced influx of Sytox Green into (a) *S. aureus* and (b) *E. coli*.

were 19.62 ± 0.07 mm, 21.68 ± 0.15 mm and 25.78 ± 0.18 mm. It has excellent antibacterial properties against Gram-negative bacteria.

3.7. Membrane permeabilization

The ability of Cu(II) complexes to disrupt and increase cell membrane permeability was evaluated by using Sytox green into *S. aureus* and *E. coli* cells. Sytox green is a green nucleic acid dye that easily penetrates the damaged plasma membrane and cannot penetrate the plasma membrane of living cells [33]. As shown in Figure 6, when treated with copper complexes, a significant fluorescent signal was present in *S. aureus* and *E. coli*, while the untreated control did not. The results indicate that copper complexes may destroy the integrity of bacterial cell membranes and induce the absorption of Sytox green.

4. Conclusion

Herein, we report three thiosemicarbazide and Cu(II) complexes with potential antiproliferative and antibacterial activity. The structure-activity relationship showed that the modification of lipophilic groups on the ligand significantly increased the biological resistance of Cu(II) complexes. The intervention of Cu(II) complexes greatly shortened the G2 phase in the cell cycle. Studies on the mechanism of apoptosis have shown that copper complexes promote early cell apoptosis by increasing the release of intracellular ROS. The inhibition zone experiment proved that the Cu(II) complexes had better inhibitory effect on Gram-negative bacteria. In addition, this study suggested that Cu(II) complexes may initially cause instability of the outer membrane/LPS, destroying the cell membrane, leading to bacterial cell lysis. These results may be beneficial for the development of new Cu(II) complexes as candidates for antitumor drugs.

Disclosure statement

The authors declare that they have no conflict of interests.

Funding

This work was supported by National Natural Science Foundation of China (81571812), Pingdingshan College PhD Startup Fund under Grant PXY-BSQD-202003; key specialized research and development breakthrough in Henan province (202102310476 and 182102310181); and A Project Funded by the Priority Academic Program Development of Jiangsu Higher Education Institutions under Grant 1107047002.

References

[1] K. Zaher, S. Malihe, M. Victoria, M. Leili, G. Elham. *Adv. Hum. Biol.*, **9**, 245 (2019).
[2] Z.J. Cai, Q. Liu. *Sci. China Life Sci.*, (2019) doi:10.1007/s11427-019-9816-1.
[3] A. Syse, M. Veenstra, B. Aagnes, S. Tretli. *Nor. J. Epidemiol.*, **22**, 109 (2012).
[4] B. Rosenberg. *Cisplatin*, **9**, (1980). doi:10.1016/B978-0-12-565050-2.50006-1
[5] D.K. Armstrong, B. Bundy, L. Wenzel, H.Q. Huang, R. Baergen, S. Lele, L.J. Copeland, J.L. Walker, R.A. Burger. *N. Engl. J. Med.*, **354**, 34 (2006).
[6] G.V. Kalayda, M. Kullmann, M. Galanski, S. Gollos. *J. Biol. Inorg. Chem.*, **22**, 1295 (2017).
[7] R.M. Wouda, S.E. Hocker, M.L. Higginbotham. *Vet. Comp. Oncol.*, **16**, 202 (2017).
[8] T.C. Johnstone, K. Suntharalingam, S.J. Lippard. *Chem. Rev.*, **116**, 3436 (2016).
[9] H. Na, T.S. Teets. *J. Am. Chem. Soc.*, **140**, 6353 (2018).
[10] K. Kumar, S. Schniper, A. González-Sarrías, A.A. Holder, N. Sanders, D. Sullivan, W.L. Jarrett, K. Davis, F. Bai, N.P. Seeram, V. Kumar. *Eur. J. Med. Chem.*, **86**, 81 (2014).
[11] V.F.S. Pape, N.V. May, G. Tamás Gál, I. Szatmári, F. Szeri, F. Fülöp, G. Szakács, É.A. Enyedy. *Dalton Trans.*, **47**, 17032 (2018).
[12] A. Fetoh, O.A. El-Gammal, G.M.A. El-Reash. *J. Mol. Struct.*, **1173**, 100 (2018).
[13] Q.Y. Yang, Q.Q. Cao, Q.P. Qin, C.X. Deng, H. Liang, Z.F. Chen. *Int. J. Mol. Sci.*, **19**, 1874 (2018).
[14] Q.Y. Yi, W.D. Li, L.S. Chen, Z.S. Bai. *BMC Infect. Dis.*, **18**, 671 (2018).
[15] V.W. Soo, B.W. Kwan, H. Quezada, I. Castillo–Juárez, B. Pérez-Eretza, S.J. García-Contreras, M. Martínez-Vázquez, T.K. Wood, R. García-Contreras. *Curr. Top. Med. Chem.*, **17**, 1157 (2017).
[16] W.X. Bi, F. Kong, X.Y. Hu, X. Cui. *Toxicol. Mech. Methods.*, **17**, 371 (2007).
[17] L.-J. Shin, J.-C. Lo, K.-C. Yeh. *Plant Physiol.*, **159**, 1099 (2012).
[18] D.B. Lovejoy, P.J. Jansson, U.T. Brunk, J. Wong, P. Ponka, D.R. Richardson. *Cancer Res.*, **71**, 5871 (2011).
[19] S.U. Parsekar, J. Fernandes, A. Banerjee, O.P. Chouhan, S. Biswas, M. Singh, D.P. Mishra, M. Kumar. *J. Biol. Inorg. Chem.*, **23**, 1331 (2018).
[20] J.X. Qi, Q. Yao, L. Tian, Y. Wang. *Eur. J. Med. Chem.*, **158**, 853 (2018).
[21] S.J. Sardroud, S.A. Hosseini-Yazdi, M. Mahdavi, M. Poupon, E. Skorepova. *Polyhedron*, **175**, 114218 (2020).
[22] S.A. Khan, P. Kumar, R. Joshi, P.F. Iqbal, K. Saleem. *Eur. J. Med. Chem.*, **43**, 2029 (2008).
[23] V. Opletalová, D.S. Kalinowski, M. Vejsová, J. Kunes, M. Pour, J. Jampílek, V. Buchta, D.R. Richardson. *Chem. Res. Toxicol.*, **21**, 1878 (2008).
[24] A.A. Ali, H. Nimir, C. Aktas, V. Huch, U. Rauch, K.H. Schäfer, M. Veith. *Organometallics*, **31**, 2256 (2012).
[25] P. Chellan, K.M. Land, A. Shokar, A. Au, S.H. An, C.M. Clavel, P.J. Dyson, C. de Kock, P.J. Smith, K. Chibale, G.S. Smith. *Organometallics*, **31**, 5791 (2012).

[26] J.X. Qi, Y.Y. Zheng, K. Qian, L. Tian, G.X. Zhang, Z. Cheng, Y.H. Wang. *J. Inorg. Biochem.*, **177**, 110 (2017).
[27] A.P. Pannu, J.R. Stevens, P.G. Plieger. *Inorg. Chem.*, **52**, 9327 (2013).
[28] L. Li, D. Liao, Z. Jiang, J.M. Mouesca, P. Rey. *Inorg. Chem.*, **45**, 7665 (2006).
[29] O.V. Dolomanov, L.J. Bourhis, R.J. Gildea, J.A.K. Howard, H. Puschmann. *J. Appl. Crystallogr.*, **42**, 339 (2009).
[30] J.D. Burton. *Methods Mol. Med.*, **110**, 69 (2005).
[31] M.Z. Sai, S.L. Zhong, Y. Tang, W.T. Ma, Y.G. Sun, D.R. Ding. *J. Appl. Polym. Sci.*, **131**, 40535 (2014).
[32] V.P. Parvathi, M. Umadevi, R. Sasikala, R. Parimaladevi, V. Ragavendran, J. Mayandi, G.V. Sathe. *Mater. Lett.*, **258**, 126775 (2020).
[33] A. Makovitzki, D. Avrahami, Y. Shai. *Proc. Natl. Acad. Sci. USA.*, **103**, 15997 (2006).
[34] P.J. Jansson, P.C. Sharpe, P.V. Bernhardt, D.R. Richardson. *J. Med. Chem.*, **53**, 5759 (2010).
[35] D.X. West, H. Gebremedhin. *Trans. Met. Chem.*, **20**, 84 (1995).
[36] Z.Y. Ma, J. Shao, W.G. Bao, Z.Y. Qiang, J.Y. Xu. *J. Coord. Chem.*, **68**, 277 (2015).
[37] L. Tom, N. Aiswarya, S.S. Sreejith, M.R.P. Kurup. *Inorg. Chim. Acta*, **473**, 223 (2018).
[38] O. Dömötör, N.V. May, K. Pelivan, T. Kiss, B.K. Keppler, C.R. Kowol, É.A.A. Enyedy. *Inorg. Chim. Acta*, **472**, 264 (2018).
[39] P. Heffeter, V.F.S. Pape, É.A. Enyedy, B.K. Keppler, G. Szakacs, C.R. Kowol. *Antioxid. Redox Signal.*, **30**, 1062 (2019).
[40] C.R. Kowol, W. Miklos, S. Pfaff, S. Hager, S. Kallus, K. Pelivan, M. Kubanik, É.A. Enyedy, W. Berger, P. Heffeter, B.K. Keppler. *J. Med. Chem.*, **59**, 6739 (2016).
[41] R. Gil-García, P. Gómez-Saiz, V. Díez-Gómez, G. Madariaga, M. Insausti, L. Lezama, J.V. Cuevas, J. García-Tojal. *Polyhedron*, **81**, 675 (2014).
[42] J. García-Tojal, R. Gil-García, V.I. Fouz, G. Madariaga, L. Lezama, M.S. Galletero, J. Borrás, F.I. Nollmann, C. García-Girón, R. Alcaraz, M. Cavia-Saiz, P. Muñiz, O. Palacios, K.G. Samper, T. Rojo. *J. Inorg. Biochem.*, **180**, 69 (2018).
[43] E.W. Ainscough, A.M. Brodie, W.A. Denny, G.J. Finlay, J.D. Ranford. *J. Inorg. Biochem.*, **70**, 175 (1998).
[44] P.J. Jansson, D.S. Kalinowski, D.J.R. Lane, Z. Kovacevic, N.A. Seebacher, L. Fouani, S. Sahni, A.M. Merlot, D.R. Richardson. *Pharmacol. Res.*, **100**, 255 (2015).
[45] A.E. Stacy, D. Palanimuthu, P.V. Bernhardt, D.S. Kalinowski, P.J. Jansson, D.R. Richardson. *J. Med. Chem.*, **59**, 4965 (2016).
[46] A.E. Stacy, D. Palanimuthu, P.V. Bernhardt, D.S. Kalinowski, P.J. Jansson, D.R. Richardson. *J. Med. Chem.*, **59**, 8601 (2016).
[47] Z. Al-Eisawi, C. Stefani, P.J. Jansson, A. Arvind, P.C. Sharpe, M.T. Basha, G.M. Iskander, N. Kumar, Z. Kovacevic, D.J.R. Lane, S. Sahni, P.V. Bernhardt, D.R. Richardson, D.S. Kalinowski. *J. Med. Chem.*, **59**, 294 (2016).
[48] Y. Yu, D.S. Kalinowski, Z. Kovacevic, A.R. Siafakas, P.J. Jansson, C. Stefani, D.B. Lovejoy, P.C. Sharpe, P.V. Bernhardt, D.R. Richardson. *J. Med. Chem.*, **52**, 5271 (2009).
[49] D.R. Richardson, D.S. Kalinowski, V. Richardson, P.C. Sharpe, D.B. Lovejoy, M. Islam, P.V. Bernhardt. *J. Med. Chem.*, **52**, 1459 (2009).
[50] A. Dobrova, S. Platzer, F. Bacher, M.N.M. Milunovic, A. Dobrov, G. Spengler, E.A. Enyedy, G. Novitchi, V.B. Arion. *Dalton Trans.*, **45**, 13427 (2016).
[51] H. Liu, M. Gong, B.A. French, G. Liao, J. Li, B. Tillman, S.W. French. *Oncotarget*, **6**, 42491 (2015).
[52] Z.X. Cao, Q.Q. Yang, H.Y. Yin, Q. Qi, H.G. Li, G.Y. Sun, H.G. Wang, W.W. Liu, J.F. Li. *Apoptosis*, **22**, 1419 (2017).
[53] Z.H. Feng, W.H. Zheng, Q. Tang, L. Cheng, H. Li, W.F. Ni, X.Y. Pan. *Apoptosis*, **22**, 1001 (2017).
[54] C. Chen, Y. Liu, Y. Liu, P. Zheng. *Cell Cycle*, **8**, 1158 (2009).
[55] Z.J. Li, S.C. Zhang, J. Zhang, M. Liu, Z.H. Liu. *Mol. Immunol.*, **46**, 3232(2009).